nature geoscience

LETTERS

PUBLISHED ONLINE: 13 JULY 2014 | DOI: 10.1038/NGEO2200

Eddy-induced variability in Southern Ocean abyssal mixing on climatic timescales

K. L. Sheen[1]*, A. C. Naveira Garabato[1], J. A. Brearley[1], M. P. Meredith[2,3], K. L. Polzin[4], D. A. Smeed[5], A. Forryan[1], B. A. King[5], J-B. Sallée[2,6], L. St. Laurent[4], A. M. Thurnherr[7], J. M. Toole[4], S. N. Waterman[8,9] and A. J. Watson[10]

The Southern Ocean plays a pivotal role in the global ocean circulation and climate[1–3]. There, the deep water masses of the world ocean upwell to the surface and subsequently sink to intermediate and abyssal depths, forming two overturning cells that exchange substantial quantities of heat and carbon with the atmosphere[4,5]. The sensitivity of the upper cell to climatic changes in forcing is relatively well established[6]. However, little is known about how the lower cell responds, and in particular whether small-scale mixing in the abyssal Southern Ocean, an important controlling process of the lower cell[7,8], is influenced by atmospheric forcing. Here, we present observational evidence that relates changes in abyssal mixing to oceanic eddy variability on timescales of months to decades. Observational estimates of mixing rates, obtained along a repeat hydrographic transect across Drake Passage, are shown to be dependent on local oceanic eddy energy, derived from moored current meter and altimetric measurements. As the intensity of the regional eddy field is regulated by the Southern Hemisphere westerly winds[9,10], our findings suggest that Southern Ocean abyssal mixing and overturning are sensitive to climatic perturbations in wind forcing.

The Southern Ocean limb of the global overturning circulation consists of two cells[4]. The upper cell involves the southward flow and upwelling of mid-depth waters of North Atlantic origin, their transformation into lighter waters within the upper layers of the Antarctic Circumpolar Current (ACC), and their subsequent return northward as mode and intermediate waters. This vertical circulation is driven by a combination of wind-driven Ekman motions, eddy-induced flows, and air–sea interaction, which sustains the diabatic near-surface water mass transformation[6,11]. In the lower cell, the southward shoaling of mid-depth waters is balanced by the production of dense waters by intense oceanic heat loss along the Antarctic margin. These dense waters sink to become the abyssal water masses that are exported northward into and across the ACC and, in the process, are transformed into less dense, shallower waters by small-scale, turbulent diabatic mixing. Ultimately, the intensity of this mixing exerts a major control on the rate at which the abyssal ocean overturns[7,12].

Observations of the spatial distribution of turbulent mixing[13–15] and idealized modelling studies[12,16] link the occurrence of Southern Ocean abyssal mixing to the breaking of internal lee waves, generated as the ACC's vigorous mesoscale eddy flows impinge on seafloor topography. The radiation and breaking of lee waves is estimated to account for a significant fraction of the dissipation of the Southern Ocean eddy field[16,17], and to support the diabatic water mass transformation closing the lower overturning cell in the abyssal ocean[7,18]. This prompts the hypothesis that Southern Ocean abyssal mixing and overturning are sensitive to the intensity of the regional eddy field and, because the eddy field is primarily energized by instabilities of the wind-forced circulation[19], to climatic perturbations in atmospheric forcing.

We address this hypothesis by analysing the temporal variability of Southern Ocean abyssal mixing and internal wave properties using a unique collection of repeat measurements of shear microstructure and density fine structure along a repeat hydrographic transect (designated SR1b), which crosses the ACC in Drake Passage (Fig. 1). These measurements include three repeat shear microstructure sections (conducted in April 2011, February/March 2012 and March 2013, under the auspices of the Diapycnal and Isopycnal Mixing Experiment in the Southern Ocean, DIMES; http://dimes.ucsd.edu), from which the spatial distribution of the rate of dissipation of turbulent kinetic energy (ϵ, a metric of the intensity of small-scale turbulence) is computed. In addition, twenty repeat density fine-structure sections (conducted quasi-annually between November 1993 and March 2013) are analysed to estimate ϵ using a fine-scale parameterization[15,20]. The results of these calculations are interpreted in the context of satellite altimetric observations of surface kinetic energy anomaly, KE_{anom}, and with reference to a 2-year (December 2009–March 2012) mooring record of KE_{anom} and abyssal internal wave shear (from which ϵ is estimated with a fine-scale parameterization analogous to that above) with daily resolution in northern Drake Passage (Fig. 1). These mooring data were also obtained as part of DIMES (ref. 21). Details of all data sets and calculations are provided in the Methods and Supplementary Information.

The temporal variability in small-scale turbulence across Drake Passage is illustrated by Fig. 2, showing profiles of ϵ and current speed for the three repeat microstructure sections. In all of the sections, turbulent dissipation in the northern half of the SR1b section is generally elevated relative to the southern half, as expected from the rougher topography in the northern region[15]. Turbulent dissipation rates to the south of the Polar Front approach open-ocean background levels ($\epsilon = O(10^{-10})\,W\,kg^{-1}$ associated with a diapycnal diffusivity of $K_\rho = O(10^{-5})\,m^2\,s^{-1}$) below the

[1]University of Southampton, National Oceanography Centre, Southampton SO14 3ZH, UK, [2]British Antarctic Survey, Cambridge CB3 0ET, UK, [3]Scottish Association for Marine Science, Oban PA37 1QA, UK, [4]Woods Hole Oceanographic Institution, 266 Woods Hole Road, Woods Hole, Massachusetts 02543-1050, USA, [5]National Oceanography Centre, Southampton SO14 3ZH, UK, [6]Laboratoire d'Océanographie et du Climat, 75252 Paris, France, [7]Lamont-Doherty Earth Observatory, Palisades, New York 10964, USA, [8]Climate Change Research Centre and ARC Centre of Excellence for Climate System Science, University of New South Wales, Sydney, New South Wales 2052, Australia, [9]University of British Columbia, Vancouver, British Columbia V6T 1Z4, Canada, [10]University of Exeter, EX4 4SB, UK. *e-mail: K.Sheen@soton.ac.uk

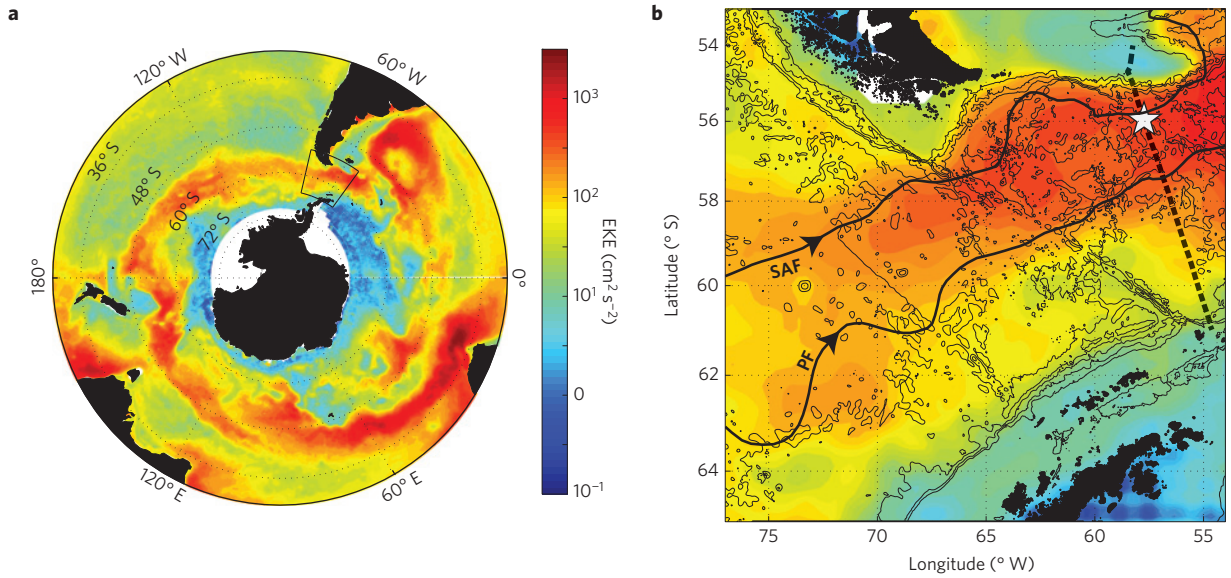

Figure 1 | Location of the DIMES experiment, the SR1b section and the DIMES mooring array. a, Altimetric surface eddy kinetic energy (EKE) across the Antarctic Circumpolar Current (ACC) (Methods) between 1993 and 2013. The outlined area indicates the region considered in this study, shown in **b**. **b**, Surface EKE in Drake Passage (coloured shading), with thin grey lines indicating isobaths at 1,000 m intervals. The dashed black line marks the SR1b section, and the white star marks the location of the DIMES mooring array. The solid black lines show the mean positions of the Subantarctic Front (SAF) and Polar Front (PF; ref. 29).

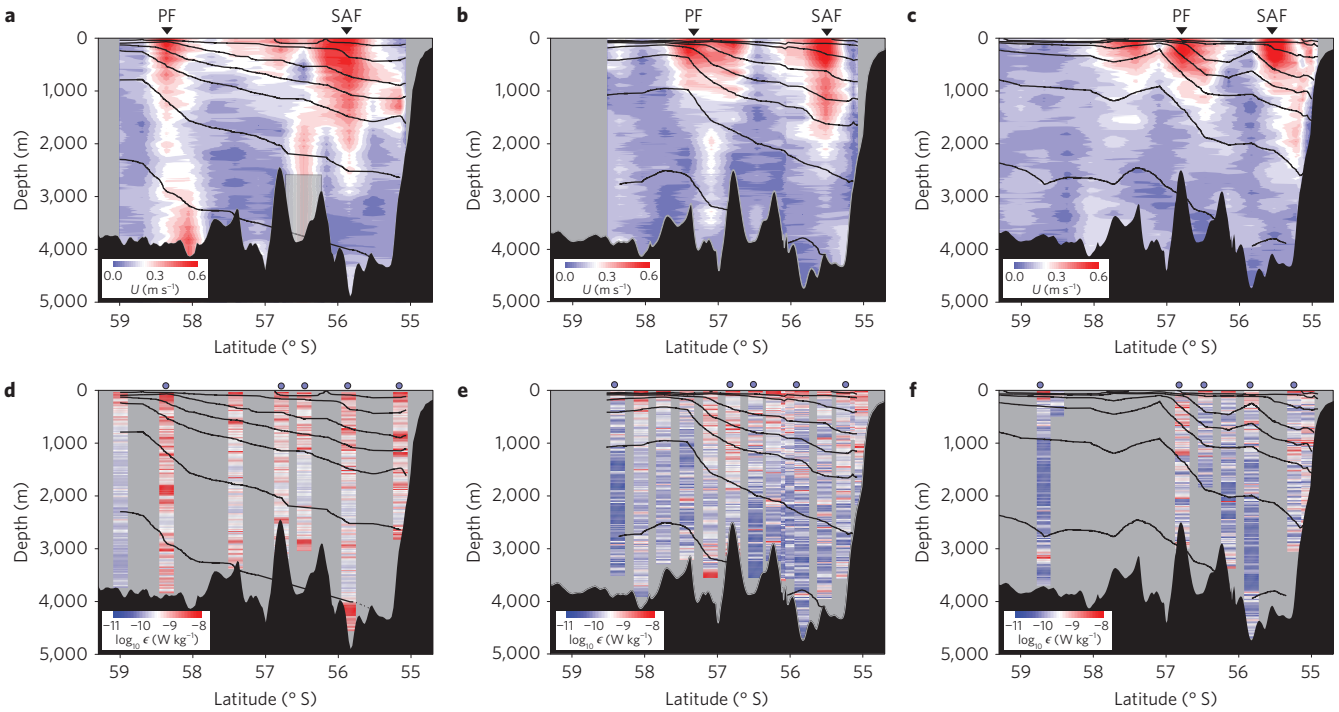

Figure 2 | Current speed and turbulent dissipation rates across three repeat microstructure sections. a–c, Lowered-ADCP (see Methods) current speed along SR1b in April 2011, February/March 2012 and March 2013. Black lines indicate neutral density surfaces every 0.2 kg m^{-3} between 26.8 kg m^{-3} and 28.2 kg m^{-3}. Solid black area denotes submarine topography. Black triangles mark the ACC fronts. No data are available in grey regions. **d–f**, Profiles of microstructure-derived ϵ (rate of dissipation of turbulent kinetic energy) for the SR1b section occupations in April 2011, February/March 2012 and March 2013. Blue circles mark the five co-located stations (Supplementary Fig. 2).

upper-ocean mixed layer, and patches of enhanced dissipation rates ($\epsilon = O(10^{-9})$ W kg^{-1}; $K_\rho = O(10^{-4})$ m^2 s^{-1}) are found consistently over the northern continental slope. Elsewhere, substantial section-to-section variations are apparent. Most significantly, in April 2011, dissipation levels to the north of the Polar Front are elevated by up to one order of magnitude ($\epsilon \sim 10^{-9}$ W kg^{-1}) relative to the other two sections ($\epsilon \sim 10^{-10}$ W kg^{-1}), and exhibit a more pronounced near-bottom enhancement. This difference occurs in association with a general intensification of near-bottom flows in April 2011, and stems from microstructure profiles collected within areas of relatively high near-bottom speed associated with the eddying frontal jets of the ACC (Supplementary Fig. 3). These observations

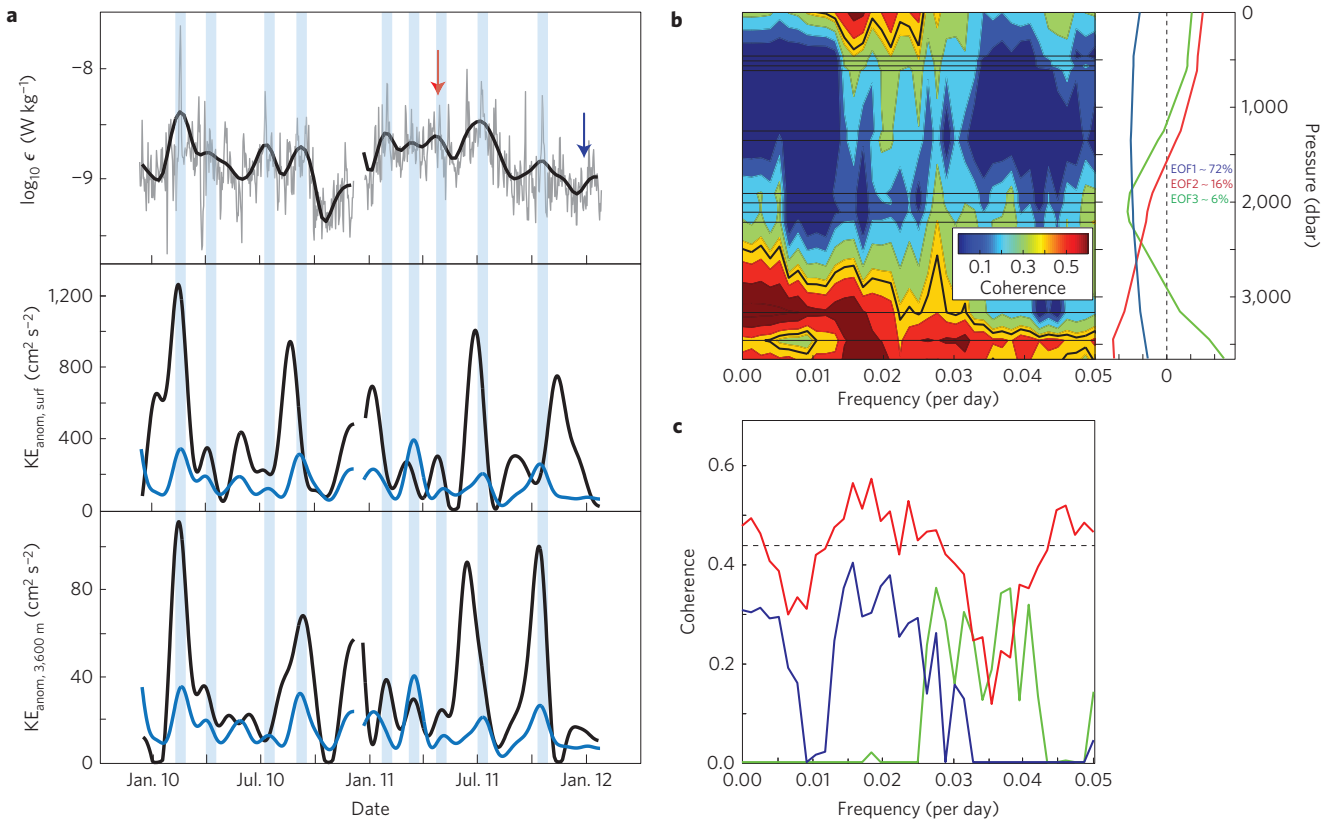

Figure 3 | Relationship between abyssal turbulent dissipation and surface and abyssal kinetic energy anomaly at the DIMES mooring site. a, Upper panel: daily (thin grey line) and 45-day low-pass-filtered (thick black line) time series of abyssal ϵ at the mooring site. Red and blue arrows mark the section occupations in April 2011 (Fig. 2a–d) and November/December 2011 (Fig. 4). Blue bars indicate maxima in the filtered ϵ series. Middle and lower panels show the filtered altimetric kinetic energy anomaly and the kinetic energy anomaly at ~3,600 m (black lines) alongside their equivalent second empirical orthogonal function (EOF) expression (blue lines). **b**, Spectral coherence between abyssal ϵ and the KE_{anom} from moored current meters, surface altimetry data and depth-mean moored ADCP velocities. Black contour indicates 95% significance level. Horizontal black lines mark pressure levels at which KE_{anom} was computed. The vertical structure of the first three complex EOF modes for the current velocity are plotted. **c**, Spectral coherence between the series of abyssal ϵ and KE_{anom} computed from EOF1 (blue), EOF2 (red) and EOF3 (green) of current velocity. Black dashed line marks the 95% significance.

suggest that changes in near-bottom eddy flow underpin the observed temporal variability of turbulent dissipation in the Drake Passage abyss, consistent with the generation and breaking of internal waves.

This interpretation is supported by two complementary lines of evidence. First, a significant correlation exists between the measured near-bottom speed and microstructure-derived abyssal dissipation for the three microstructure sections (Supplementary Information), pointing to a link between the two variables. Although correlation does not prove causality, application of wave radiation theory[15] to the observations of near-bottom flow during the three repeat microstructure sections confirms that the intensification of the flow in April 2011 is sufficient to account for the order-of-magnitude enhancement in dissipation documented at that time (Supplementary Fig. 4). Second, the 2-year mooring record of fine-structure-derived abyssal dissipation in northern Drake Passage exhibits a lognormal standard deviation of 0.3 and a range of two orders of magnitude ($\epsilon = 2 \times 10^{-10}$ W kg^{-1} to $\epsilon = 2.3 \times 10^{-8}$ W kg^{-1}, Fig. 3a), and is significantly correlated and energetically consistent with the near-bottom eddy flow speed[21]. The influence of tidal flows was found not to exert a primary control on mixing rates at this location[21]. The mooring time series of abyssal dissipation also reveals that the April 2011 microstructure section was obtained during a 6-month period in which dissipation was enhanced by a factor of ~2.5 relative to early 2012, immediately before the microstructure transect occupation in February/March of that year.

The changes in near-bottom eddy flow modulating variations in abyssal turbulence are not exclusively a deep-ocean phenomenon, but are part of a mode of eddy variability that is evident throughout the water column. This is illustrated by the analysis of the vertical structure in the spectral coherence between abyssal dissipation and KE_{anom} (Methods) at the DIMES mooring site. Fluctuations in abyssal dissipation with periods of 1–3 months, characteristic of the eddy field, are significantly coherent with KE_{anom} changes in the deepest ~1,000 m of the water column and in the surface altimetry, but incoherent with fluctuations in mid-depth KE_{anom} (Fig. 3b and Supplementary Information). This pattern of coherence reflects the first-baroclinic modal structure of the current velocity field that is typically exhibited by eddy motions with a prominent near-bottom and surface manifestation and which corresponds to the second empirical orthogonal function (EOF2). The abyssal dissipation is therefore significantly correlated not only with near-bottom KE_{anom}, but also with altimetry-derived surface KE_{anom} and KE_{anom} derived from EOF2 of the velocity field (Fig. 3 and Supplementary Information). The energization of first-baroclinic mode eddy flows is a predicted effect of baroclinic instability[22], and may be expected to enhance abyssal dissipation through the promotion of internal wave generation by intensified near-bottom currents[12,14,15,17] (despite accounting for only 16% of the total KE_{anom} variance, EOF2 contributes 44% of the time-integrated bottom KE_{anom}, compared with 27% for EOF1; see Supplementary Information).

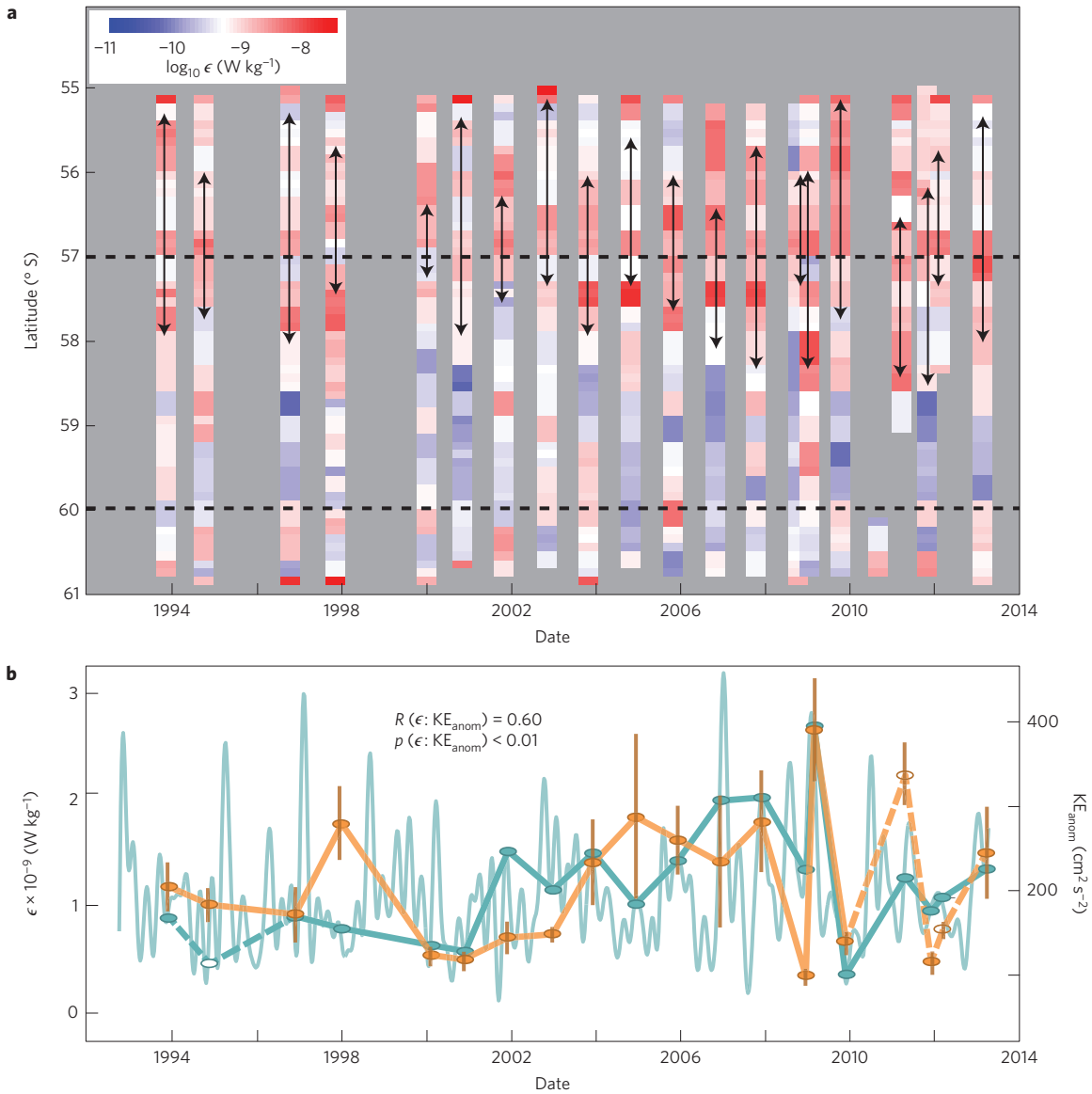

Figure 4 | Decadal variability in turbulent dissipation rate and EKE along the SR1b section in eastern Drake Passage. a, Mean ϵ within 2 km of the sea bed along SR1b as a function of latitude and time. Black arrows indicate the region between the Subantarctic Front and Polar Front; that is, where the difference in geopotential anomaly between 100 db and 1,000 dbar is 4.5 to 8.5 $m^3\ kg^{-1}$; dashed lines show the latitude limits of the area used to construct the time series in **b**. **b**, Time series of surface KE_{anom} averaged over a 3° square centred on 58.5° S, 57.5° W and filtered with a 90-day low-pass Butterworth filter (pale blue line). The darker blue line/ovals highlight times of SR1b occupations. Open ovals/dashed lines mark when the European Remote-Sensing (ERS) satellite was in its geodetic mission (Supplementary Information). The orange line/ovals indicate abyssal ϵ averaged between 57° S and 60°; vertical dark orange bars show standard errors. Open ovals/dashed lines indicate times when some CTD stations (see Methods) in the averaging region were not occupied (**a**).

The existence of a surface footprint of near-bottom eddy activity in Drake Passage allows us to assess the mechanisms underpinning variability in abyssal turbulent dissipation over longer, climatically relevant timescales (years to decades). A 20-year time series of fine-structure-derived abyssal dissipation (Fig. 4a) reveals a similar spatial pattern to that in the microstructure data (Fig. 2): consistently elevated dissipation ($\epsilon \sim 3 \times 10^{-9}\ W\ kg^{-1}$) near the northern edge of Drake Passage, over the South American continental slope; lower dissipation ($\epsilon \sim 3 \times 10^{-10}\ W\ kg^{-1}$) south of 58.5° S, where topography is relatively smooth and eddy variability is weak; and highly variable dissipation in between (the topographic height variance, computed using multibeam bathymetry data, is 70–240 m on the south of the section compared with 210–320 m north of 57.5° S (ref. 15)). There is a sharp transition between intense and weak dissipation that migrates meridionally between section occupations and spans the 57° S–58.5° S latitude range. Significantly, this transition tracks closely the position of the meandering Polar Front jet, as might be expected if abyssal dissipation were modulated by eddy flows with both surface and bottom expressions. The same relationship is evident in a comparison between time series of fine-structure-derived abyssal dissipation within the latitude band of the Polar Front and altimetric surface KE_{anom} (Fig. 4b). Surface KE_{anom} is highly variable, but a record of KE_{anom} values extracted at the times of occupation of the SR1b section exhibits a significant correlation with ϵ ($R = 0.6$ and $p < 0.01$, with a mean and standard error of 0.57 and 0.18 respectively, determined by bootstrapping with 1,000 samples, Supplementary Fig. 5) that is robust to modest variations in the latitude band over which data are averaged. Note that the reduction

in fine-structure-derived dissipation and surface KE_{anom} between April 2011, February/March 2012 and March 2013 is consistent with the microstructure observations (Fig. 2).

Global maps of altimetric surface eddy kinetic energy (EKE, the average of KE_{anom} over many eddy timescales) indicate that the SR1b transect is embedded within a region of elevated EKE (Fig. 1). It has been shown that EKE in this and other ACC areas around major topographic obstacles is modulated by changes in wind forcing on interannual-to-interdecadal timescales, largely associated with major climatic modes such as the Southern Annular Mode and El Niño/Southern Oscillation[9,10] (Supplementary Fig. 7). This climatic modulation is evident in EKE averaged over the wider Drake Passage region; however, the nature of the eddy field's response to a forcing perturbation is both non-local and highly patchy on length scales comparable to those of the eddies themselves (O(100 km)) (ref. 10). As a result, a relationship between large-scale forcing and EKE along the SR1b section (or any other similarly sized line across the ACC) is not expected, and the evolution of local KE_{anom} is dominated by stochastic eddy variability with timescales of weeks to months (Fig. 4b). However, because the fundamental dynamics linking eddy flows to deep-ocean turbulent dissipation is common to all ACC regions characterized by rough topography[12–15], the sensitivity of Southern Ocean EKE to changes in forcing is indicative of a climatic modulation of abyssal mixing in the region.

This study represents the first evidence that variability of Southern Ocean abyssal mixing on timescales of months to decades is modulated by mesoscale eddies, consistent with the mechanism of breaking internal waves generated as deep-reaching eddy flows impinge on seafloor topography. The Southern Ocean eddy field is primarily energized by instabilities of the wind-forced ACC (ref. 19) and, as such, its kinetic energy is sensitive to climatic perturbations in the Southern Hemisphere westerlies[9,10]. It thus follows that the intensity of Southern Ocean abyssal mixing is likely to be similarly reactive to climatic modulation. Motivated by the recent and projected interdecadal intensification of the westerlies[23,24], many authors have investigated the eddy-mediated response of the upper cell of global overturning to changes in Southern Ocean wind forcing[25,26]. As Southern Ocean abyssal mixing is a major driver of the lower overturning cell[7,12,27], our findings suggest that this circulation is likely to be regulated by the westerlies, and that the dynamical coupling between winds, eddies and abyssal mixing unveiled here must be factored into investigations of the climatic evolution of deep-ocean overturning.

Methods

Estimates of turbulent dissipation rates along the SR1b section. The rate of turbulent kinetic energy dissipation, ϵ, along three occupations of the SR1b section was determined using free-falling vertical microstructure profilers. Assuming isotropy, $\epsilon = 15\nu/2(\overline{\partial u/\partial z})^2$, where ν is the molecular viscosity and $\partial u/\partial z$ is the vertical velocity shear[28]. Velocity shear variances were calculated every 0.5 m, using shear spectra computed over bin widths of 1 s and integrated between 1 Hz and the spectral minimum between 10 Hz and 25 Hz (or 10 Hz and 100 Hz for $\epsilon > 10^{-7}$ W kg^{-1}). The sampling rate of the vertical microstructure profilers is 512 Hz. In addition, indirect estimates of turbulent dissipation were obtained by applying a fine-scale parameterization[20] to conductivity–temperature–depth (CTD)-derived strain for twenty repeat SR1b hydrographic sections (further details are given in Supplementary Information and ref. 15).

DIMES mooring array data and analysis. A 10.5 km by 10.5 km array of six moorings was deployed close to the northern end of the SR1b line between 12 December 2009 and 5 March 2012 (ref. 21; Fig. 1). Velocity measurements from 12 current meters installed at depths ranging from 425 m to 3,600 m in the central mooring, and from a downward-looking acoustic Doppler current profiler (ADCP) ensonifying the depth range 2,800–3,300 m in the same mooring, were analysed to characterize the vertical structure of $KE_{anom} = [(u-\overline{u})^2 + (v-\overline{v})^2]/2$, where u is the zonal velocity, v is the meridional velocity and the overbar indicates the time mean over the mooring deployment period (that is, eddy here refers to any time-varying flow with mesoscale spatial scales, be it a ring or a meander). The mooring was also instrumented with SeaBird MicroCAT CTDs at the same vertical levels as the current meters. Velocity shear data from the moored ADCP were used to estimate a 2-year time series of ϵ at the mooring site (full details are documented in ref. 21). The data gap in December 2010 is associated with the mooring turn-around half-way through the deployment.

Computation of surface kinetic energy anomaly. The zonal, u, and meridional, v, components of the surface geostrophic velocity anomaly were calculated from satellite altimetry-derived sea-level anomaly gradients, and the surface kinetic energy anomaly, $KE_{anom} = [(u-\overline{u})^2 + (v-\overline{v})^2]/2$, was computed, where the overbar represents the time mean since the start of December 1993 (20-year altimetric time series), corresponding to the time of the first SR1b hydrographic section occupation.

Received 24 January 2014; accepted 9 June 2014; published online 13 July 2014

References

1. Toggweiler, J. R. & Russell, J. Ocean circulation in a warming climate. *Nature* **451,** 286–288 (2008).
2. Skinner, L. C., Fallon, S., Waelbroeck, C., Michel, E. & Barker, S. Ventilation of the deep Southern Ocean and deglacial CO_2 rise. *Science* **328,** 1147–1151 (2010).
3. Rintoul, S. & Naveira Garabato, A. C. *Ocean circulation and Climate: A 21st Century Perspective. International Geophysics*, Ch. 18, 471–491 (Academic, 2013).
4. Lumpkin, R. & Speer, K. Global ocean meridional overturning. *J. Phys. Oceanogr.* **37,** 2550–2562 (2007).
5. Lauderdale, J. M., Naveira Garabato, A. C., Oliver, K. I. C., Follows, M. J. & Williams, R. G. Wind-driven changes in Southern Ocean residual circulation, ocean carbon reservoirs and atmospheric CO_2. *Clim. Dyn.* **41,** 2145–2164 (2013).
6. Marshall, J. & Speer, K. Closure of the meridional overturning circulation through Southern Ocean upwelling. *Nature Geosci.* **5,** 171–180 (2012).
7. Ito, M. & Marshall, J. Control of lower-limb overturning circulation in the Southern Ocean by diapycnal mixing and mesoscale eddy transfer. *J. Phys. Oceanogr.* **38,** 2832–2845 (2008).
8. Nikurashin, M. & Vallis, R. A theory of deep stratification and overturning circulation in the ocean. *J. Phys. Oceanogr.* **41,** 485–502 (2011).
9. Meredith, M. P. & Hogg, A. M. Circumpolar response of Southern Ocean eddy activity to a change in the Southern Annular Mode. *Geophys. Res. Lett.* **33,** L16608 (2006).
10. Morrow, R., Ward, M. L., Hogg, A. M. & Pasquet, S. Eddy response to Southern Ocean climate modes. *J. Geophys. Res.* **115,** C10030 (2010).
11. Sloyan, B. & Rintoul, S. R. The Southern Ocean limb of the global deep overturning circulation. *J. Phys. Oceanogr.* **31,** 143–173 (2001).
12. Nikurashin, M., Vallis, R. & Adcroft, A. Routes to energy dissipation for geostrophic flows in the Southern Ocean. *Nature Geosci.* **6,** 48–51 (2013).
13. St. Laurent, L. *et al.* Turbulence and diapycnal mixing in Drake Passage. *J. Phys. Oceanogr.* **42,** 2143–2152 (2012).
14. Waterman, S., Naveira Garabato, A. C. & Polzin, K. L. Internal waves and turbulence in the Antarctic Circumpolar Current. *J. Phys. Oceanogr.* **43,** 259–282 (2013).
15. Sheen, K. L. *et al.* Rates and mechanisms of turbulent dissipation and mixing in the Southern Ocean: Results from the Diapycnal and Isopycnal Mixing Experiment in the Southern Ocean (DIMES). *J. Geophys. Res.* **118,** 1–19 (2013).
16. Nikurashin, M. & Ferrari, R. Radiation and dissipation of internal waves generated by geostrophic motions impinging on small-scale topography: Theory. *J. Phys. Oceanogr.* **40,** 1055–1074 (2010).
17. Scott, R. B., Goff, J. A., Naveira Garabato, A. C. & Nurser, A. J. G. Global rate and spectral characteristics of internal gravity wave generation by geostrophic flow over topography. *J. Geophys. Res.* **116,** C09029 (2011).
18. Nikurashin, M. & Ferrari, R. Overturning circulation driven by breaking internal waves in the deep ocean. *Geophys. Res. Lett.* **40,** 3133–3137 (2013).
19. Ferrari, R. & Wunsch, C. Ocean circulation kinetic energy: Reservoirs, sources, and sinks. *Annu. Rev. Fluid Mech.* **41,** 253–282 (2009).
20. Gregg, M. C., Sanford, T. B. & Winkel, D. P. Reduced mixing from the breaking of internal waves in equatorial waters. *Nature* **422,** 513–515 (2003).
21. Brearley, J. A., Sheen, K. L., Naveira Garabato, A. C., Smeed, D. A. & Waterman, S. Eddy-induced modulation of turbulent dissipation over rough topography in the Southern Ocean. *J. Phys. Oceanogr.* **43,** 2288–2308 (2013).
22. Venaille, A. M., Vallis, G. K. & Smith, K. S. Baroclinic turbulence in the ocean: Analysis with primitive equation and quasigeostrophic simulations. *J. Phys. Oceanogr.* **41,** 1605–1606 (2011).
23. Yin, J. A consistent poleward shift of the storm tracks in simulations of 21st century climate. *Geophys. Res. Lett.* **32,** L18701 (2005).

24. Thompson, W. J. & Solomon, S. Interpretation of recent Southern Hemisphere climate change. *Science* **296,** 895–899 (2002).
25. Hallberg, R. & Gnanadesikan, A. The role of eddies in determining the structure and response of the wind-driven Southern Hemisphere overturning: Results from the modeling eddies in the Southern Ocean (MESO) project. *J. Phys. Oceanogr.* **36,** 2232–2252 (2006).
26. Abernathey, R., Marshall, J. & Ferreira, D. Dependence of Southern Ocean overturning on wind stress. *J. Phys. Oceanogr.* **41,** 2261–2278 (2011).
27. Stanley, G. J. & Saenko, O. A. Bottom-enhanced diapycnal mixing driven by mesoscale eddies: Sensitivity to wind energy supply. *J. Phys. Oceanogr.* **44,** 68–85 (2014).
28. Oakey, N. S. Determination of the rate of dissipation of turbulent energy from simultaneous temperature and velocity shear microstructure measurements. *J. Phys. Oceanogr.* **12,** 256–271 (1982).
29. Orsi, A. H., Whitworth, T. III, Worth, D. & Nowlin, W. D. Jr On the meridional extent and fronts of the Antarctic Circumpolar Current. *Deep-Sea Res. I* **42,** 641–673 (1995).

Acknowledgements

The DIMES experiment is supported by the Natural Environment Research Council (NERC) of the UK and the US National Science Foundation. K.L.S. is supported by NERC. We are grateful to J. Ledwell, A. Bogdanoff, P. Courtois, K. Decoteau, D. Evans and X. Liang for their help in data collection and acknowledge the valuable assistance and hard work of the crew and technicians on the RRS *James Cook*, the RRS *James Clark Ross* and the RV *Thomas G. Thompson*. We also thank A. Thompson who provided many helpful comments, and E. Murowinski, R. Lueck and F. Wolk from Rockland Scientific for their support in microstructure data analysis.

Author contributions

K.L.S. conducted most of the data analysis. A.C.N.G. and K.L.S. conceived the idea for the work and wrote the manuscript. J.A.B. processed the mooring current velocity data and computed the mooring turbulent dissipation time series. K.L.S., J.A.B., A.C.N.G., A.F. and L.S.L. collected and processed microstructure data. B.A.K. was instrumental in collecting hydrographic data along the repeat SR1b section. A.M.T. collected and processed lowered-ADCP data for the three DIMES SR1b sections. A.C.N.G., J.M.T., D.A.S. and A.J.W. conceived and directed the DIMES project and along with J-B.S. planned research cruises. M.P.M., K.L.P., D.A.S., J-B.S. and S.N.W. gave analytical and conceptual advice throughout the project.

Additional information

Supplementary information is available in the online version of the paper. Reprints and permissions information is available online at www.nature.com/reprints. Correspondence and requests for materials should be addressed to K.L.S.

Competing financial interests

The authors declare no competing financial interests.